Numerical modelling of elastomers using the boundary element method

M. T. Bayliss *, A. El-Zafrany

School of Engineering, Cranfield University, Cranfield,

Bedfordshire, MK43 OAL, UK

Tel: 01234 754643

Fax: 01234 750425

E-mail: m.t.bayliss@cranfield.ac.uk

Summary

The FEM analysis of hyper elastic, elastomeric materials has been formulated and implemented for various material models (strain energy functions) over the years. More recently the analysis of elastomeric materials has been attempted in the boundary element method. This has been achieved by the addition of non-linear domain terms to the basic linear boundary element equation. These non-linear domain terms require the evaluation of the displacement derivative components directly from displacement derivative boundary integral equations. In the solution to the boundary problem it is required to regularize the different types of singularities occurring in

*Funded by the Engineering and Physical Sciences Research Council, UK.

the system of non-linear boundary integral equations. This paper discusses the necessary theory for the boundary element method as applied to elastomers and presents a comparison between semi-analytical and numerical solutions for various test cases.

Keywords: Elastomers; BEM; Mooney-Rivlin; Singular integrals

Nomenclature

Acronym

BIE Boundary integral equation

CPV Cauchy principal value

DBIE Derivative boundary integral equation

FEM Finite element method

PK Piola Kirchhoff

p Modified Piosson's ratio

Greek

μ Shear modulus

1 Introduction

Two recent papers by Al-Gahtani et al. [1], and Polizzotto [2] give the most up to date and relevant work on the application of the BEM to the stress analysis of hyperelastic and incompressible materials. Polizzotto discusses the Galerkin boundary element formulation with regard to elastomers. The generation of the non-linear domain integrals is mentioned with the additional problem of singular integrals. Another more complex approach to evaluating the non-linear domain terms is given by Guiggiani [3] where the CPV term generated by the CPV theorem is expanded as a Taylor series in terms of polar coordinates.

Al-Qahtani et al. [1] elaborate on this subject giving some detail on the evaluation of singular and hypersingular integrals by means of integration by parts and the use of the divergence theorem. They also give details of an iterative solution procedure assuming a constant 1^{st} PK stress distribution within the non-linear domain terms present in each BIE.

In this paper a BIE approach for elastomers is presented with a second order isoparametric stress distribution assumed within the integration cells. In addition a simplified approach for the singularity regularization required to solve the basic system of boundary displacements and tractions is given. The regularization is simplified in comparison to similar work by AL-Gahtani et al. Specifically, for this research two closely related approaches are given for removal of $1/r^2$ hyper-singularities in the domain integral terms of the DBIE. The hypersingular kernel function is isolated and evaluated either to be zero by applying the mean value theorem and integration by parts, or of constant value for domain quadrature points by the application of the CPV theorem. In contrast Al-Gahtani et al. state that the domain integrals are converted to boundary integrals where the singularity will not occur as the quadrature point will always be inside the problem domain and not on the boundary. Other more elaborate approaches exist for regularization of $1/r$ and $1/r^2$ domain integral singularities such as the approach used by Guiggiani et al. [3], as mentioned earlier.

An iterative technique for the evaluation of the hydrostatic pressure to use within the Mooney-Rivlin derived non-linear stress expression for the case of plane strain is discussed. For validation a comparison is made between semi-analytical and numerical results for various test cases.

The case of uniaxial extension of a unit cube of elastomeric material under plane strain is presented. In order to validate the theory for non-uniform stress fields a plane stress test case for a thick walled pressurized cylinder is also given.

2 The non-linear BIE for elastomers

The starting point for the derivation of the non-linear BIE is the equation of internal equilibrium referred to undeformed co-ordinates and based on 1^{st} PK stress. Note that the domain loading terms have been removed.

$$\sum_{\beta=1}^{2} \frac{\partial \sigma_{\beta\alpha}}{\partial x_\beta} = 0 \tag{1}$$

The equilibrium equation can be written in terms of linear and non-linear stresses, with the non-linear stresses taking on the appearance of domain loading terms, hence:

$$\sum_{\beta=1}^{2} \frac{\partial \sigma^{l}_{\beta\alpha}}{\partial x_\beta} + f^{nl}_{\alpha} = 0 \qquad f^{nl}_{\alpha} = \sum_{\beta=1}^{2} \frac{\partial \sigma^{nl}_{\beta\alpha}}{\partial x_\beta} \tag{2}$$

The Galerkin weighted-residual approach is then applied to equation 2 to obtain the inverse weighted-residual expression as follows:

$$\begin{gathered}\oint_{\Gamma} \left(T^{l}_{x} u^{*} + T^{l}_{y} v^{*}\right) \mathrm{d}\Gamma - \oint_{\Gamma} \left(T^{*}_{x} u + T^{*}_{y} v\right) \mathrm{d}\Gamma + \iint_{\Omega} \left(f^{nl}_{x} u^{*} + f^{nl}_{y} v^{*}\right) \mathrm{d}\Omega + \\ \iint_{\Omega} \left[u \left(\frac{\partial \sigma^{*}_{x}}{\partial x} + \frac{\partial \tau^{*}_{yx}}{\partial y} \right) + v \left(\frac{\partial \tau^{*}_{xy}}{\partial x} + \frac{\partial \sigma^{*}_{y}}{\partial y} \right) \right] \mathrm{d}\Omega = 0\end{gathered} \tag{3}$$

The last domain integral in equation 3 can be simplified by introducing another equilibrium equation for the fundamental stress terms and substituting Dirac delta function and load per unit thickness products for the fundamental loads. Using the properties of the Dirac delta function the following expression is obtained:

$$
\begin{aligned}
C_i u_i e_x + C_i v_i e_y + \oint_\Gamma \left(T_x^* u + T_y^* v\right) \mathrm{d}\Gamma = \\
\oint_\Gamma \left(T_x^l u^* + T_y^l v^*\right) \mathrm{d}\Gamma + \iint_\Omega \left(f_x^{nl} u^* + f_y^{nl} v^*\right) \mathrm{d}\Omega
\end{aligned}
\tag{4}
$$

The C_i components are the Dirac delta coefficients. It can be shown that the fundamental solutions can be expressed in terms of kernel functions and the fundamental load components [4]. Hence the BIE for a single direction component can be written from equation 4 as:

$$
C_i u_{\alpha i} + \sum_{\beta=1}^{2} \oint_\Gamma F_{\beta\alpha} u_\beta \mathrm{d}\Gamma = \sum_{\beta=1}^{2} \oint_\Gamma G_{\beta\alpha} T_\beta^l \mathrm{d}\Gamma + \sum_{\beta=1}^{2} \iint_\Omega G_{\beta\alpha} f_\beta^{nl} \mathrm{d}\Omega \tag{5}
$$

A further simplification can be achieved if the non-linear domain term is integrated by parts and the resulting linear and non-linear traction boundary integral terms combined for the total traction to give:

$$
C_i u_{\alpha i} + \sum_{\beta=1}^{2} \oint_\Gamma F_{\beta\alpha} u_\beta \mathrm{d}\Gamma = \sum_{\beta=1}^{2} \oint_\Gamma G_{\beta\alpha} T_\beta \mathrm{d}\Gamma - \sum_{\gamma=1}^{2} \sum_{\beta=1}^{2} \iint_\Omega \left[\sigma_{\beta\gamma}^{nl} \frac{\partial G_{\gamma\alpha}}{\partial x_\beta}\right] \mathrm{d}\Omega \tag{6}
$$

Equation 6 is the basic non-regularized BIE of displacement.

3 BIE regularization

The $log(r)$ singularity in the second boundary integral term can be dealt with by means of logarithmic quadrature [4]. Note:

$$
r = \sqrt{(x - x_i)^2 + (y - y_i)^2} \tag{7}
$$

where (x, y) is the field point and (x_i, y_i) is the source point. The $1/r$ strong singularity contained in the first boundary integral term in the $F_{\beta\alpha}$ kernel function is removed by applying the CPV theorem [5]. The resulting CPV term can either be shown to be zero on a smooth boundary or inside the problem domain, or evaluated explicitly using rigid body motion for the case of a source point on a boundary corner. The resulting regularized BIE is of the following form:

$$\sum_{\beta=1}^{2} C_{\alpha\beta_i} u_{\beta_i} + \sum_{\beta=1}^{2} \oint_{\Gamma'} F_{\beta\alpha} u_\beta \mathrm{d}\Gamma = \sum_{\beta=1}^{2} \oint_{\Gamma} G_{\beta\alpha} T_\beta \mathrm{d}\Gamma - \sum_{\gamma=1}^{2} \sum_{\beta=1}^{2} \iint_\Omega \left[\sigma_{\beta\gamma}^{nl} \frac{\partial G_{\gamma\alpha}}{\partial x_\beta} \right] \mathrm{d}\Omega \quad (8)$$

where

$$\oint_{\Gamma'} F_{\beta\alpha} u_\beta \mathrm{d}\Gamma \equiv \lim_{\epsilon \to 0} \oint_{\Gamma - \Gamma_\epsilon} F_{\beta\alpha} u_\beta \mathrm{d}\Gamma \quad (9)$$

Γ_ϵ represents the boundary of a small circle with radius ϵ centered at the source point (x_i, y_i) which is on the problem domain boundary. The domain integral term in equation 8 contains a $1/r$ singularity. Re-writing the domain term in equation 8:

$$\sum_{\gamma=1}^{2} \sum_{\beta=1}^{2} \iint_\Omega \frac{\partial G_{\gamma\alpha}}{\partial x_\beta} \sigma_{\beta\gamma}^{nl} \mathrm{d}\Omega = \sum_{\gamma=1}^{2} \sum_{\beta=1}^{2} \left[\iint_\Omega \frac{\partial G_{\gamma\alpha}}{\partial x_\beta} \left[\sigma_{\beta\gamma}^{nl} - \left(\sigma_{\beta\gamma}^{nl} \right)_i \right] \mathrm{d}\Omega + \iint_\Omega \frac{\partial G_{\gamma\alpha}}{\partial x_\beta} \left(\sigma_{\beta\gamma}^{nl} \right)_i \mathrm{d}\Omega \right] \quad (10)$$

Applying integration by parts:

$$\sum_{\gamma=1}^{2} \sum_{\beta=1}^{2} \iint_\Omega \frac{\partial G_{\gamma\alpha}}{\partial x_\beta} \sigma_{\beta\gamma}^{nl} \mathrm{d}\Omega = \sum_{\gamma=1}^{2} \sum_{\beta=1}^{2} \left[\iint_\Omega \frac{\partial G_{\gamma\alpha}}{\partial x_\beta} \left[\sigma_{\beta\gamma}^{nl} - \left(\sigma_{\beta\gamma}^{nl} \right)_i \right] \mathrm{d}\Omega + \oint_\Gamma G_{\gamma\alpha} l_\beta \left(\sigma_{\beta\gamma}^{nl} \right)_i \mathrm{d}\Gamma \right] \quad (11)$$

and defining:

$$\bar{T}_x^{nl} = l \left(\sigma_x^{nl} \right)_i + m \left(\tau_{yx}^{nl} \right)_i \quad (12)$$

$$\bar{T}_y^{nl} = l \left(\tau_{xy}^{nl} \right)_i + m \left(\sigma_y^{nl} \right)_i \quad (13)$$

Enabling equation 8 to be written as:

$$\sum_{\beta=1}^{2} C_{\alpha\beta_i} u_{\beta_i} + \sum_{\beta=1}^{2} \oint_{\Gamma'} F_{\beta\alpha} u_\beta \mathrm{d}\Gamma = \sum_{\beta=1}^{2} \oint_{\Gamma} G_{\beta\alpha} \left[T_\beta - \bar{T}_\beta^{nl}\right] \mathrm{d}\Gamma - \sum_{\gamma=1}^{2} \sum_{\beta=1}^{2} \iint_{\Omega} \frac{\partial G_{\gamma\alpha}}{\partial x_\beta} \left[\sigma_{\beta\gamma}^{nl} - \left(\sigma_{\beta\gamma}^{nl}\right)_i\right] \mathrm{d}\Omega \tag{14}$$

Equation 14 represents a fully regularized form of the displacement BIE. The final domain term can be shown to have no singularity using the CPV theorem. Therefore it can be seen that the domain integral in equation 14 has no CPV value.

4 Regularized DBIE

When the derivative is taken the regularized displacement derivative form of equation 14 will contain two $1/r^2$ hyper-singularity integral terms. The first will be due to the first boundary integral term involving the kernel function derivative $\frac{\partial F_{\beta\alpha}}{\partial x_\delta}$. The second will be due to the domain integral term involving the double derivative $\frac{\partial^2 G_{\gamma\alpha}}{\partial x_\delta \partial x_\beta}$ kernel which generates the $1/r^2$ singularity. Taking the singularity due to the derivative kernel $\frac{\partial F_{\beta\alpha}}{\partial x_\delta}$ first, replacing the modified Dirac delta term with the corresponding $F_{\beta\alpha}$ integral in equation 14 the following expression is obtained:

$$\sum_{\beta=1}^{2} \oint_{\Gamma'} F_{\beta\alpha} \left(u_\beta - u_{\beta_i}\right) \mathrm{d}\Gamma = \sum_{\beta=1}^{2} \oint_{\Gamma} G_{\beta\alpha} \left[T_\beta - \bar{T}_\beta^{nl}\right] \mathrm{d}\Gamma - \sum_{\gamma=1}^{2} \sum_{\beta=1}^{2} \iint_{\Omega} \frac{\partial G_{\gamma\alpha}}{\partial x_\beta} \left[\sigma_{\beta\gamma}^{nl} - \left(\sigma_{\beta\gamma}^{nl}\right)_i\right] \mathrm{d}\Omega \tag{15}$$

Differentiating equation 15 with respect to $x_{\delta i}$ and using kernel function identities the following equation can be obtained:

$$\sum_{\beta=1}^{2} C_{\beta\alpha_i} \frac{\partial u_{\beta_i}}{\partial x_{\delta i}} = \sum_{\beta=1}^{2} \oint_{\Gamma'} \frac{\partial F_{\beta\alpha}}{\partial x_{\delta i}} \left(u_\beta - u_{\beta_i}\right) \mathrm{d}\Gamma - \sum_{\beta=1}^{2} \oint_{\Gamma} \frac{\partial G_{\beta\alpha}}{\partial x_{\delta i}} \left[T_\beta - \bar{T}_\beta^{nl}\right] \mathrm{d}\Gamma + \sum_{\gamma=1}^{2} \sum_{\beta=1}^{2} \iint_{\Omega} \frac{\partial^2 G_{\gamma\alpha}}{\partial x_\delta \partial x_\beta} \left[\sigma_{\beta\gamma}^{nl} - \left(\sigma_{\beta\gamma}^{nl}\right)_i\right] \mathrm{d}\Omega \tag{16}$$

Which is a fully regularized displacement derivative BIE. The first boundary integral term has been shown by developed software to be regularized for the $1/r^2$ singularity in the $\frac{\partial F_{\beta\alpha}}{\partial x_{\delta i}}$ kernel function as long as the problem boundary nodes and post solution BIE source points are coincident. The second boundary integral in equation 16 has a $1/r$ singularity in the $\frac{\partial G_{\beta\alpha}}{\partial x_{\delta i}}$ kernel function which after the application of the CPV theorem can be shown to have no CPV term. Consider the final domain term in equation 16 and apply the CPV theorem:

$$\sum_{\gamma=1}^{2}\sum_{\beta=1}^{2}\iint_{\Omega}\frac{\partial^2 G_{\gamma\alpha}}{\partial x_\delta \partial x_\beta}\left[\sigma_{\beta\gamma}^{nl}-\left(\sigma_{\beta\gamma}^{nl}\right)_i\right]\mathrm{d}\Omega =$$

$$\lim_{\varepsilon\to 0}\sum_{\gamma=1}^{2}\sum_{\beta=1}^{2}\left[\iint_{\Omega-\Omega_\varepsilon}\frac{\partial^2 G_{\gamma\alpha}}{\partial x_\delta \partial x_\beta}\left[\sigma_{\beta\gamma}^{nl}-\left(\sigma_{\beta\gamma}^{nl}\right)_i\right]\mathrm{d}\Omega+\iint_{\Omega_\varepsilon}\frac{\partial^2 G_{\gamma\alpha}}{\partial x_\delta \partial x_\beta}\left[\sigma_{\beta\gamma}^{nl}-\left(\sigma_{\beta\gamma}^{nl}\right)_i\right]\mathrm{d}\Omega\right] \tag{17}$$

Taking the last domain integral in equation 17 and applying the mean value theorem followed by integration by parts the following is obtained:

$$\left[\sigma_{\beta\gamma}^{nl}-\left(\sigma_{\beta\gamma}^{nl}\right)_i\right]\lim_{\varepsilon\to 0}\oint_{\Gamma_\varepsilon} l_\delta\frac{\partial G_{\gamma\alpha}}{\partial x_\delta}\mathrm{d}\Gamma \equiv \left[\sigma_{\beta\gamma}^{nl}-\left(\sigma_{\beta\gamma}^{nl}\right)_i\right]\lim_{\varepsilon\to 0}\oint_{0}^{2\pi} l_\delta\frac{\partial G_{\gamma\alpha}}{\partial x_\delta}\quad \varepsilon\mathrm{d}\theta \tag{18}$$

Hence, when the source and field points are coincident the $1/\varepsilon$ singularity is cancelled by the ε term and the $\left[\sigma_{\beta\gamma}^{nl}-\left(\sigma_{\beta\gamma}^{nl}\right)_i\right]$ factor. A slightly different approach can be taken to regularizing the final domain integral term starting from the following partially regularized derivative B.I.E:

$$\begin{aligned}&\sum_{\beta=1}^{2}C_{\alpha\beta_i}\frac{\partial u_\beta}{\partial x_{\delta i}}+\sum_{\beta=1}^{2}\oint_{\Gamma'}\frac{\partial F_{\beta\alpha}}{\partial x_{\delta i}}\left(u_\beta-u_{\beta_i}\right)\mathrm{d}\Gamma = \\ &-\sum_{\beta=1}^{2}\oint_{\Gamma}\frac{\partial G_{\beta\alpha}}{\partial x_{\delta i}}T_\beta\mathrm{d}\Gamma+\sum_{\gamma=1}^{2}\sum_{\beta=1}^{2}\iint_{\Omega}\left[\sigma_{\beta\gamma}^{nl}\frac{\partial^2 G_{\gamma\alpha}}{\partial x_\delta \partial x_\beta}\right]\mathrm{d}\Omega\end{aligned} \tag{19}$$

The CPV theorem can be applied to the final domain term followed by the use of integration by parts and the mean value theorem. Defining:

$$J_{\gamma\alpha\delta\beta}=\frac{\partial^2 G_{\gamma\alpha}}{\partial x_\delta \partial x_\beta}\qquad T_{\gamma\alpha\delta\beta}=\frac{\partial G_{\gamma\alpha}}{\partial x_\beta}l_\delta\qquad \iint_{\Omega'}=\iint_{\Omega-\Omega_\varepsilon} \tag{20}$$

Table 1: Displacement derivative free terms.

$T_{1111} = -\frac{(5-8p)}{16\mu(1-p)}$	$T_{1211} = 0$	$T_{2111} = 0$	$T_{2211} = -\frac{(7-8p)}{16\mu(1-p)}$
$T_{1112} = 0$	$T_{1212} = \frac{1}{16\mu(1-p)}$	$T_{2112} = \frac{1}{16\mu(1-p)}$	$T_{2212} = 0$
$T_{1121} = 0$	$T_{1221} = \frac{1}{16\mu(1-p)}$	$T_{2121} = \frac{1}{16\mu(1-p)}$	$T_{2122} = 0$
$T_{1122} = -\frac{(7-8p)}{16\mu(1-p)}$	$T_{1222} = 0$	$T_{2122} = 0$	$T_{2222} = -\frac{(5-8p)}{16\mu(1-p)}$

hence the alternative regularized DBIE is of the form:

$$\sum_{\beta=1}^{2} C_{\alpha\beta_i}\frac{\partial u_\beta}{\partial x_{\delta i}} + \sum_{\beta=1}^{2}\oint_{\Gamma'}\frac{\partial F_{\beta\alpha}}{\partial x_{\delta i}}\left(u_\beta - u_{\beta_i}\right)\mathrm{d}\Gamma = -\sum_{\beta=1}^{2}\oint_{\Gamma}\frac{\partial G_{\beta\alpha}}{\partial x_{\delta i}}T_\beta \mathrm{d}\Gamma + \lim_{\varepsilon\to 0}\sum_{\gamma=1}^{2}\sum_{\beta=1}^{2}\left[\iint_{\Omega'}\sigma^{nl}_{\beta\gamma}J_{\gamma\alpha\delta\beta}\mathrm{d}\Omega + \left(\sigma^{nl}_{\beta\gamma}\right)_i\oint_{\Gamma_\varepsilon}T_{\gamma\alpha\delta\beta}\mathrm{d}\Gamma\right] \tag{21}$$

The value of the CPV free term integrals can be evaluated for internal domain cell points and are summarised in table 1.

5 Plane stress and strain cases

It can be seen that for both the BIE and the DBIE the 1^{st} PK stress components are required. The 1^{st} PK stress references undeformed Lagrangian co-ordinates and can be related to the 2^{nd} PK stress in terms of the deformation gradient matrix $\underline{G}$ as follows:

$$\underline{\sigma} = \underline{G}\,\underline{S} \tag{22}$$

It can be shown [6] that the constitutive relationship between the 2^{nd} PK stress and the state of deformation can be derived as a function of the right Cauchy-Green tensor $\underline{C}$ and the hydrostatic pressure at a point, thus:

$$\underline{S} = B_1\underline{I} + B_2\underline{C} + B_3\underline{C}^{-1} - \rho J\underline{C}^{-1} \tag{23}$$

where B_1, B_2 and B_3 are coefficients in terms of the strain invariants of $\underline{C}$ and ρ is the hydrostatic pressure. Therefore it is necessary to evaluate the in plane displacement derivatives in order to populate the right Cauchy-Green matrix $\underline{C}$. The C_{33} component value must be evaluated having considered the type of stress analysis as follows.

For plane strain it is the case that the C_{33} component is unity. But the computational difficulty that there is no stress boundary condition for the solution of the hydrostatic pressure at a point also arises. This would also be the case for the more general three dimensional case. Therefore another set of simultaneous equations is required, covering each boundary node.

The weighted residual approach can be used on the pressure/deformation compatibility equation to derive a system of simultaneous equations which can be solved for the hydrostatic pressure in a manner similar to the FEM.

The bulk modulus K is not only a function of the strain energy model but also a function of Poisson's ratio ν. Since elastomers have a Poisson's ratio close to 0.5 a $(1 - 2\nu)$ factor appears in the denominator of the Mooney-Rivlin derived bulk modulus expression. Hence the value of K is highly susceptible to the arbitrary choice of Poisson's ratio value. In the absence of compressibility data for a given elastomer an additional corrective iteration is required on the hydrostatic pressure system of equations.

For plane stress if it is assumed that the material is incompressible then the determinant of the Right-Green tensor $\underline{C}$ must be unity, hence the C_{33} component value can be found. In addition the hydrostatic pressure can be obtained using the constitutive equations and the zero out of plane stress boundary condition.

6 Validation test cases

6.1 Patch test

Three patch test meshes were run for this test case, representing domain cell mesh densities of 2x2, 4x4 and 8x8 elements. All meshes represent a $1\,cm^3$ cube of elastomeric material with Mooney-Rivlin coefficients $C_1 = 505.6$ and $C_2 = -70.6$ (curve fitted from Treloar [7] test data). The axial load used was 500 N. All meshes were constrained along the nodes on the left hand edge in the axial direction and restrained vertically at the bottom left hand node. Hence a uniform stress field was obtained.

Figure 1 shows the plane strain validation results for stress verses deformation. In figure 2 the highest mesh density BEM, FEM and constant stress interpolation BEM results are plotted with the semi-analytical results. All the numerical cases except the constant interpolation BEM results converged for the full load. The FEM case shows the best agreement with the semi-analytical solution. The BEM case shows some divergence from the semi-analytical case at the higher strains.

Figure 2 shows the plane strain convergence results for the three mesh densities used. It can be seen that the divergence from the semi-analytical and the BEM results appears unaffected by mesh density and hence some other factor must be involved.

6.2 Pressurised thick walled cylinder

For additional validation of non-uniform stress fields the case of a thick walled pressurised cylinder was modelled. The cylinder was defined in Cartesian coordinates using two planes of symmetry so that only one quarter of the cylinder was meshed.

Two FEM and BEM meshes of 4x4 and 8x8 domain cell mesh density were created and run to test for convergence of the results. An internal pressure of $10\,\frac{N}{cm^2}$ was used.

Figure 3 shows the plane stress validation stress results for the BEM, FEM and BEM constant domain cell meshes of 8x8 element density together with the semi-analytical results. Agreement between all the numerical cases and the semi-analytical solution for the stresses at internal radial positions is good, as can be seen from the figure. Some inaccuracy appears for the hoop and radial stresses nearer the internal cylinder surface where the corner nodes occur. The BEM and the BEM constant stress interpolation cases gave the results closest to the semi-analytical solution for the hoop stress at the internal surface. The BEM case also gives the best results at the internal surface for the radial stress. The BEM results show the most accurate hoop stress at the external cylinder surface. All the numerical approaches give an accurate zero radial stress at the internal cylinder surface. The convergence results shown in figure 4 seem to indicate that hoop and radial stress inaccuracies at the inner surface are not strongly dependent on mesh density.

7 Conclusions

The need to iterate on the hydrostatic pressure for plane strain when calculating the $1^{st}PK$ stress at source points is something which is not commented on in the literature. This is due to the arbitrary choice of Poisson's ratio resulting in an inaccurate bulk modulus. The solution to this problem in this work was to iterate on the hydrostatic pressure at boundary nodes with prescribed traction until the calculated stresses equal the prescribed tractions.

As can be seen from the results in section 6 the developed program clearly converges to finite strains for all the test cases investigated. It can be seen that for the patch test results the FEM program does give the best agreement with the semi-analytical results. The BEM results by comparison increasingly diverge from those of the semi-analytical solution as the load and strain increase. This could be due to the increased numerical complexity and hence greater rounding and digitising effects. It was mentioned that there are two alternative regularization approaches that can be used for the domain integral term in the DBIE. In the developed program these two approaches were both coded, however no discernable difference in program results were observed between the two methods. The results contained in this paper show that the regularization approach used for the non-linear BIE and DBIE equations for rubber allow for convergence and acceptable results.

References

[1] H. J. Al-Gahtani and N. J. Altiero, Application of the boundary element method to rubber elasticity, *Appl. Math. Modelling.*, 20:654-661, 1996.

[2] C. Polizzotto, A symmetric galerkin boundary/domain element methods for finite elastic deformations, *Comput. Meth. Appl. Mech. Engrg.*, 189:481-514, 2000.

[3] M. Guiggiani, G. Krishnasary and T. J. Rudolphi, A general algorithm for the numerical solution of hypersingular boundary integral equations, *ASME Journal of Applied Mechanics*, 59:604-614, 1992.

[4] A. El-Zafrany, *Techniques of the boundary element method*, Ellis Horwood Ltd, 1993.

[5] R. P. Kanwal, *Linear integral equations*, Academic press inc., 1971.

[6] M. A. Crisfield, *Non-linear finite element analysis of solids and structures*, John Wiley and Sons, 1997.

[7] L. R. G. Treloar, *The physics of rubber elasticity*, Oxford University Press, England, 2nd edition, 1958.

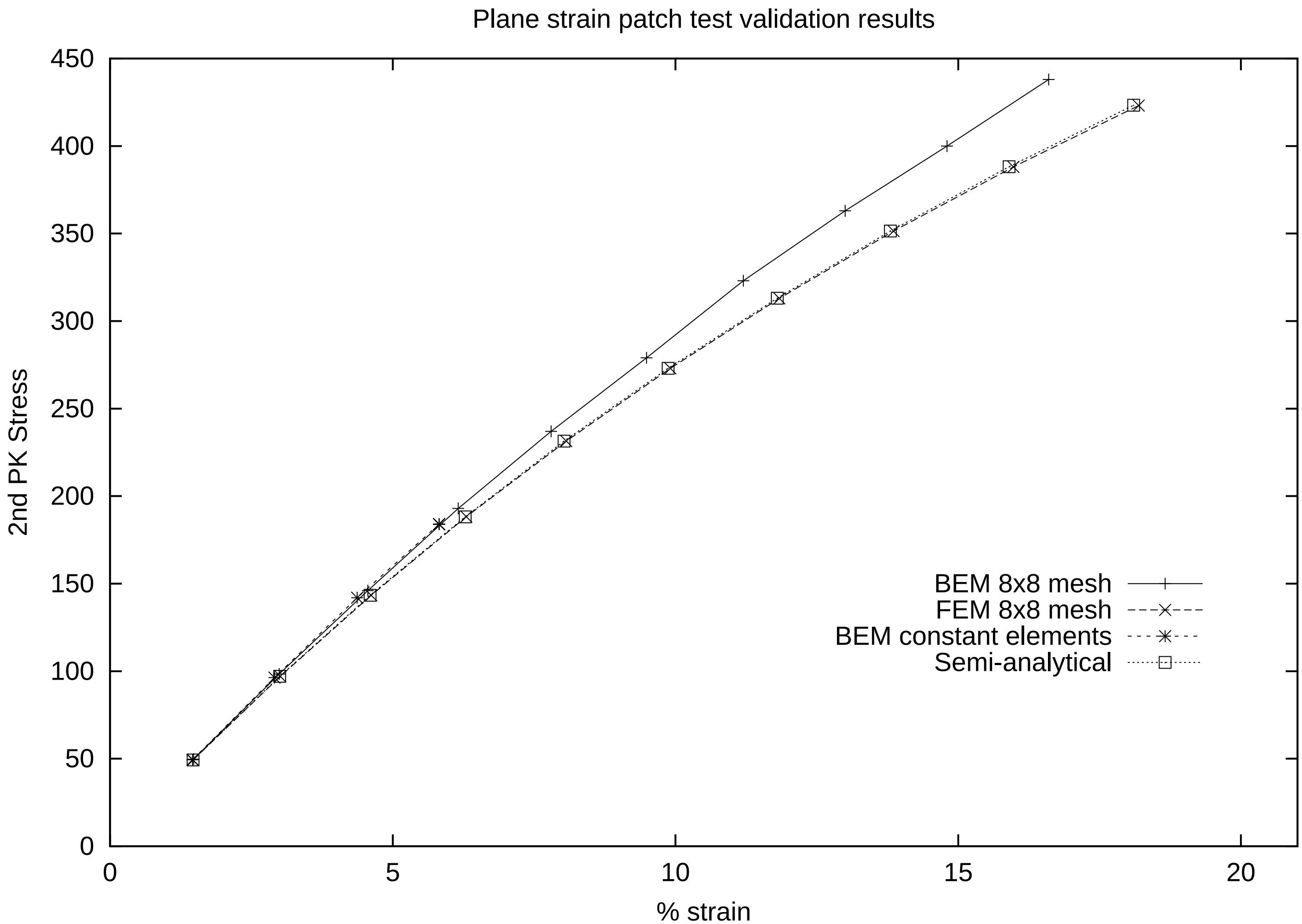
Plane strain patch test validation results
2nd PK Stress
% strain
0
50
100
150
200
250
300
350
400
450
0
5
10
15
20
BEM 8x8 mesh
FEM 8x8 mesh
BEM constant elements
Semi-analytical

Figure 1:

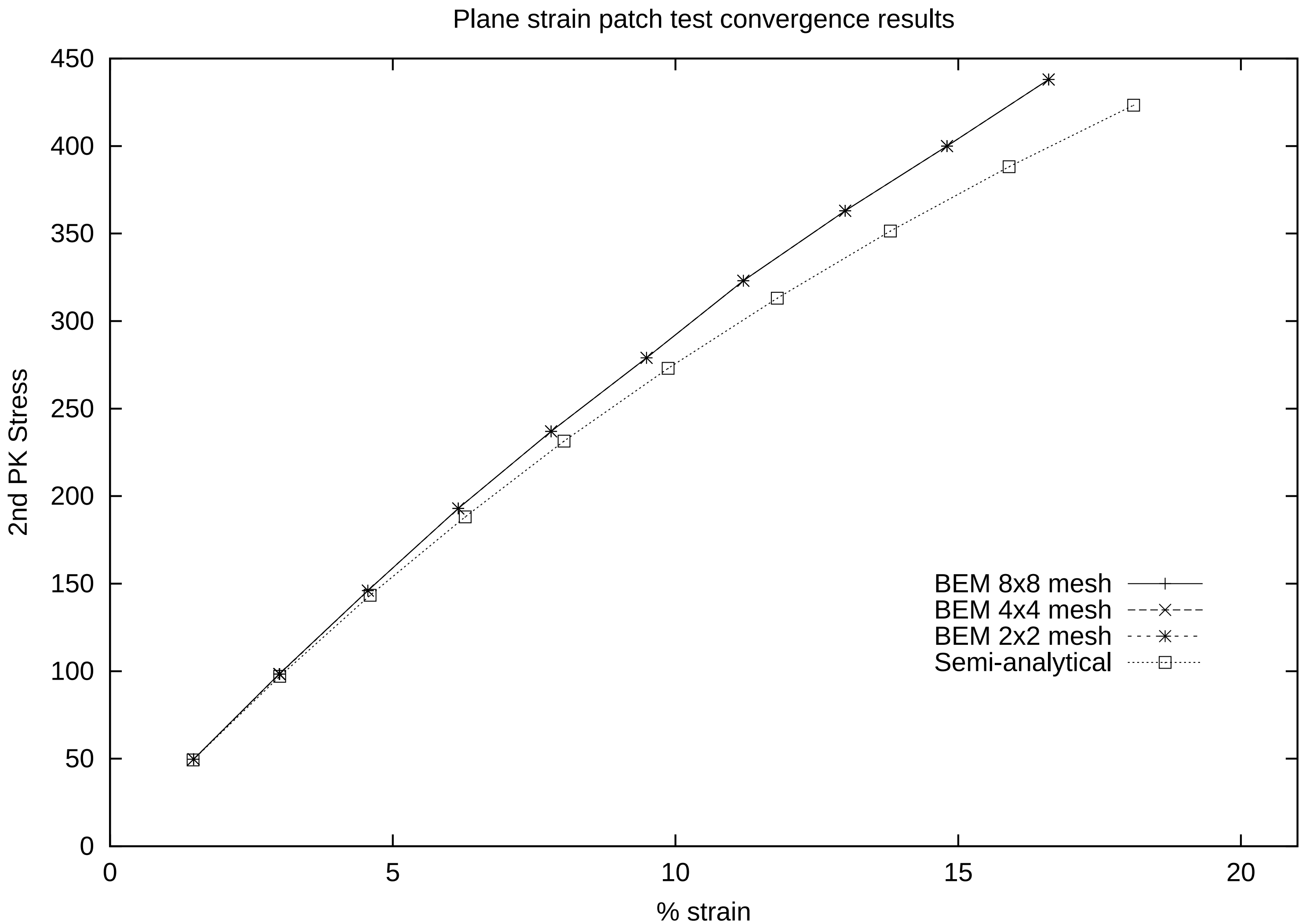

Plane strain patch test convergence results
2nd PK Stress
% strain
0
50
100
150
200
250
300
350
400
450
0
5
10
15
20
BEM 8x8 mesh
BEM 4x4 mesh
BEM 2x2 mesh
Semi-analytical

Figure 2:

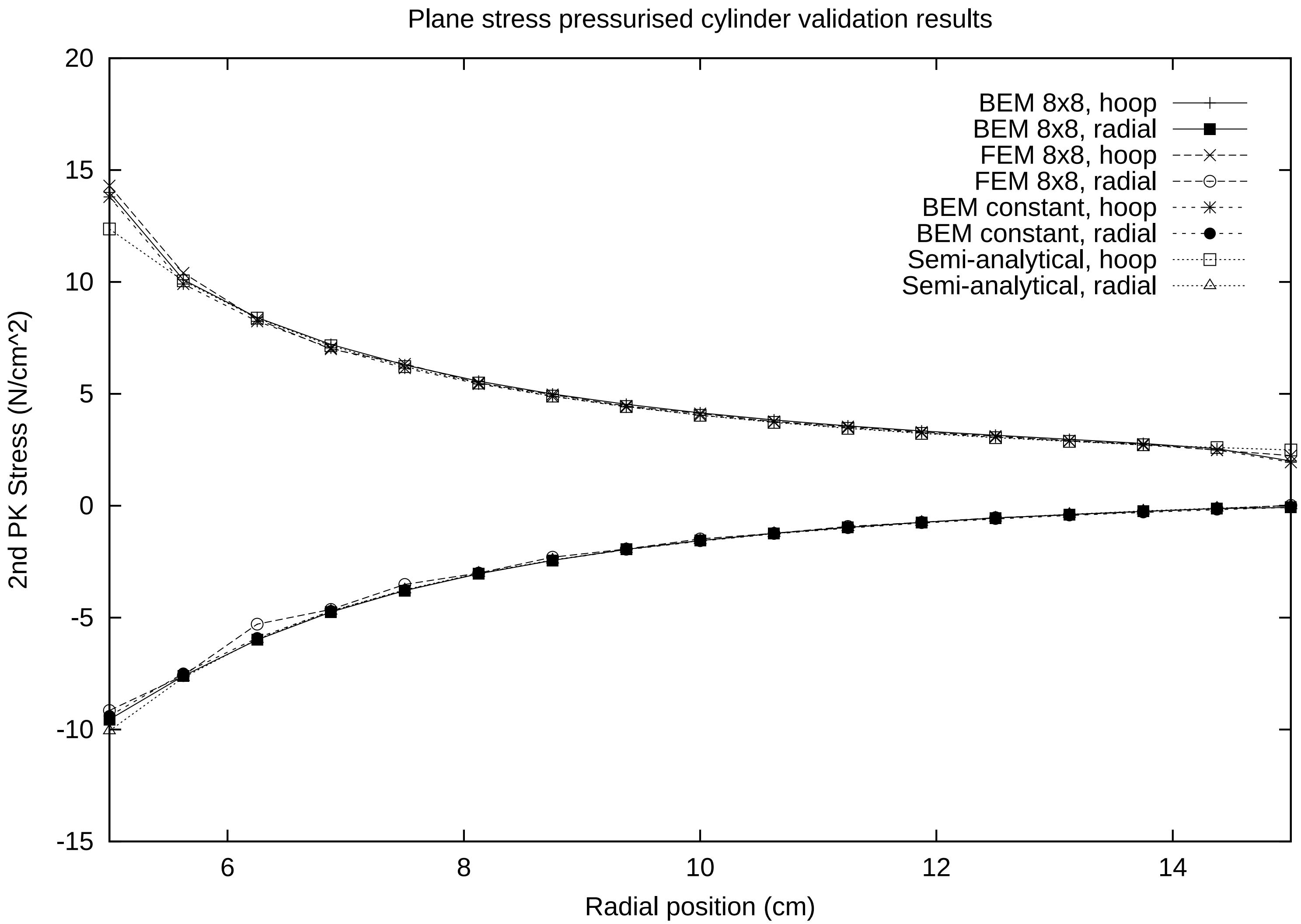
Plane stress pressurised cylinder validation results
2nd PK Stress (N/cm^2)
Radial position (cm)
BEM 8x8, hoop
BEM 8x8, radial
FEM 8x8, hoop
FEM 8x8, radial
BEM constant, hoop
BEM constant, radial
Semi-analytical, hoop
Semi-analytical, radial
20
15
10
5
0
-5
-10
-15
6
8
10
12
14

Figure 3:

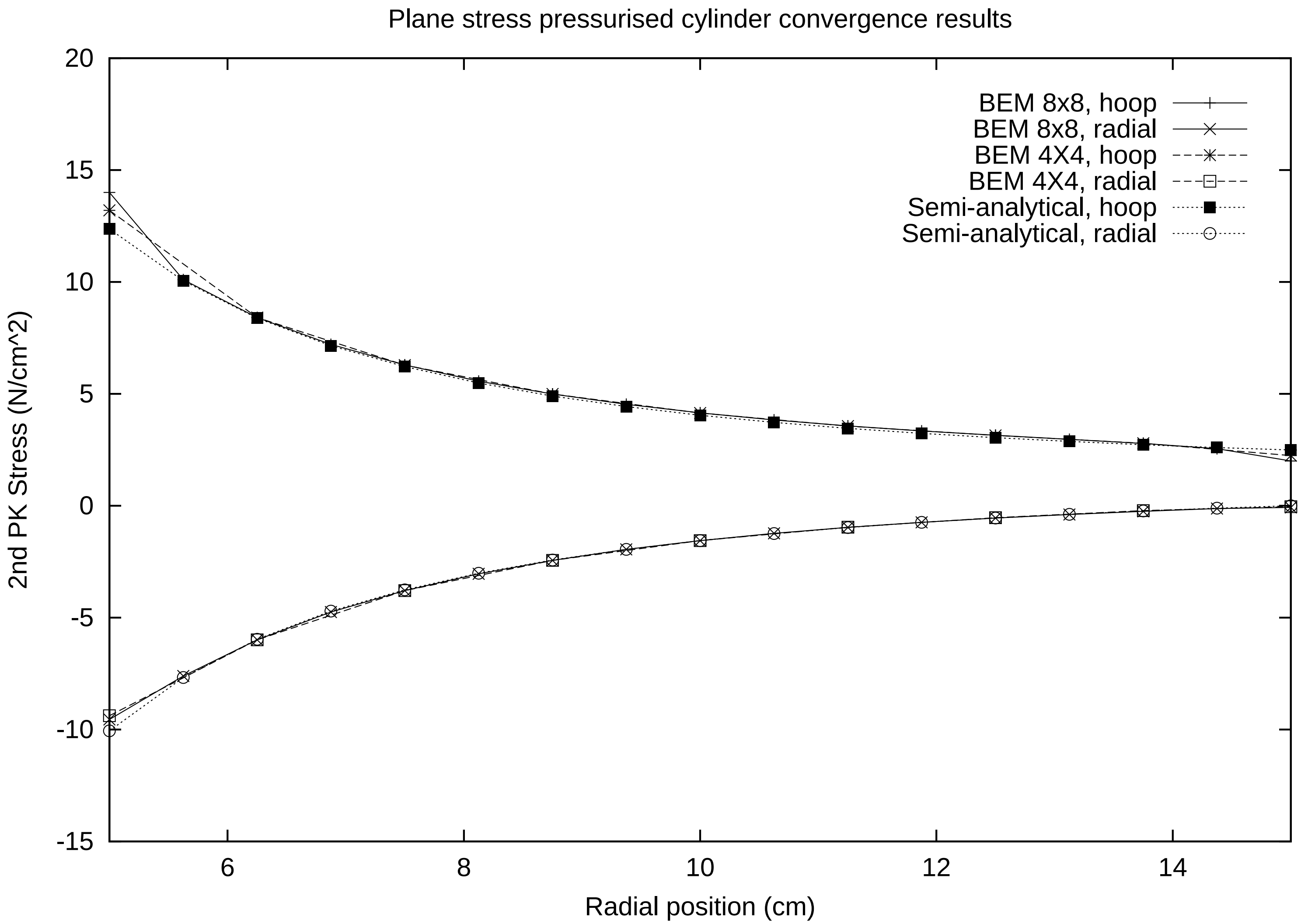
Plane stress pressurised cylinder convergence results
20
15
10
5
0
-5
-10
-15
6
8
10
12
14
Radial position (cm)
2nd PK Stress (N/cm^2)
BEM 8x8, hoop
BEM 8x8, radial
BEM 4X4, hoop
BEM 4X4, radial
Semi-analytical, hoop
Semi-analytical, radial

Figure 4: